Nickel-Based Superalloy Layer Deposited on AISI H13 Hot Tool Steel Base Metal Using Explosion Cladding Process

M. R. Khanzadeh Gharah Shiran *[1], H. Bakhtiari [2], S. A. A. Akbari Mousavi [3], A. Amadeh [4], Gh. Liaghat [5]

[1] Department of Material Engineering, Science and Research Branch, Islamic Azad University, Tehran, Iran
[2] Department of Materials Engineering, Najafabad Branch, Islamic Azad University, Najafabad, Iran
[3, 4] School of Metallurgy and Materials Engineering, Faculty of Engineering, University of Tehran, Tehran, Iran
[5] Faculty of Engineering, Tarbiat Modares University, Tehran, Iran

Abstract

An experimental test was carried out to explosively clad solution annealed Inconel 718 superalloy on quench-tempered AISI H13 hot tool steel. A wavy with vortices interface geometry was obtained from this experiment. A gradual change in the wavelength along the direction of welding was observed which was due to a change in the impact angle, following the plate contacts. In this paper, the experiment was simulated by the use of ABAQUS version 6.9 finite element software. The Williamsburg equations of state and Johnson- Cook constitutive equation were used to model the behavior of the explosive and plates, respectively. The numerical result showed that high localized plastic deformation was produced at the bond interface. Pressure magnitude was high enough to create deformation twins and slip lines in the vicinity of Inconel interface to accommodate the plastic deformation caused by shock wave velocity. SEM observation showed that the number of thin melt pockets produced in front of vortices at the interface of Inconel 718 was higher than that of AISI H13 steel. The reason was attributed to the difference between the thermal conductivity of welded alloys. The change of hardness was found to be more severe in superalloy than in steel.

Keywords: Explosive cladding; Plastic deformation; Deformation twin; Vortices.

1. Introduction

Hot forging dies are constantly under fatigue, wear, and plastic deformation, thermal and mechanical forces in service [1-3]. Such dies are usually made of hot tool steels and are used in quench-tempered conditions. Chromium type of hot tool steel such as AISI H13 are usually used under such sever condition due to having a combination of wear resistance, resistance to softening at high temperatures, toughness, and resistance to thermal and mechanical shocks [4]. In order to reduce the erosion and wear of hot forged steel, the hot tool steel is cladded with high hardness and strength materials. Nickel-base superalloys are usually used as the surface layer to maintain the corrosion resistance and strength of the die at high temperatures [5]. Surfacing processes are often performed by the fusion arc welding methods. Welding methods with the lowest heat input, dilutions, segregations, residual stresses, and distortions have shown the best results like deformation of the joint interface, improvement of tensile- shear strength, hardness and toughness, reduction of localized molten zone and intermetallic compounds at the joint interface [6].
However, surfacing of the hot tool steel by the use of fusion welding is very difficult due to its high carbon and alloying elements. Therefore, it is usually required special prudence such as controlling preheat and post weld treatments, cooling rate, choose of low hydrogen type electrode and low dilution welding procedures [5, 6].
Moreover, in the surfacing of the nickel base superalloy with the fusion welding processes, the problems such as segregation of alloying elements, precipitation, and hot crack sensitivity are raised upon solidification [7-9]. Explosion cladding is a solid state welding process where the cladding is accomplished by accelerating of one of the components (flyer plate) at high velocity toward a base plate in a predetermined stand-off distance by the use of chemical low explosives [10]. Contrary to fusion welding methods; explosion cladding does not exhibit dilution between the cladding layer and the parent plate and therefore it is possible to join metals that may exhibit hot crack sensitivity under the appropriate operational parameters. In addition, it is possible to reach full

**Corresponding author*
Email: M.khanzadeh@iaumajlesi.ac.ir
Address: Department of Material Engineering, Science and Research Branch, Islamic Azad University, Tehran, Iran
1. Assistant Professor
2. M.Sc.
3. Professor
4. Professor
5. Professor

compactness in the coating and avoid the formation of brittle intermetallic components at the bonding interface [11]. Explosive welding as a high strain rate process can create the shock wave that travels in the materials. Advancing the shock wave front in metals can create lattice defect which in turn alter the microstructure and mechanical properties [12]. Explosive welding parameters such as impact velocity, collision point velocity, dynamic collision angle, stand-off distance and the explosive ratio can also be effective on the microstructure and morphology of the interface [13, 14]. The process could be simulated using finite element method and the most aspects of the welding process could be obtained. A new approach in the simulation of explosive welding of the plates is expressed by the use of Williamsburg equation of state to simulate low explosive materials [15, 16]. New studies in the simulation have been carried out by Akbari Mousavi et al [17]. They examined the material nonlinearity due to plasticity and strain rate numerically, and using the finite element method, analyzed the large displacements by nonlinear differential equations. Their results showed that the dynamic angle of collisions plays an important role in the formation of the jets. Measuring the velocity of the jet and the jet thickness in their simulation were in a good agreement with experimental relations, and they have suggested that the change of the velocity profile and deformation of materials are responsible for the corrugated interface. In another simulation by Akbar Mousavi et al [18], on the previous research materials, the simulation results showed that the shear stresses in the base and flying metals have different signs, and in the case of having the same signs, no band was developed. Also, the values of shear stresses in the found band joints were higher than a certain threshold, and there is a certain shear stress threshold for connecting. Al-Hassani et al [19], have investigated the impact of a flying plate on the connection requirements in explosive welding and collision of plates using flying plates with flat, U- and V- shapes and the practical results with a gas gun. His simulation results showed that in these vortex-like regions, the density values are greater than the density values of the surrounding areas, thus, density distribution has a convex shape with a maximum within the vortex-shape zones. These results suggest that a state of high density or high strain, i.e. a high-pressure state is generated in deformed vortex-like zones, and they are consistent with the empirical fact that melting occurs in the center of the vortex-like zone for high collisional energy in explosive welding. Grignon et al [20] investigated explosive welding of 6061 Al-T0 alloy to alloy 6061 Al- T0. They performed their tests with preliminary stopping angles of 4, 8, 6 and 12 degrees and concluded that the welding quality is better for 10°. Since there are complicated and different phenomena in this process such as explosions, rapid collision of metals, plastic deformation of metals and creation of high temperatures and pressures in a very short time in the collisional zone, and owing to the fact that it is difficult to measure some of the data directly, it seems that the numerical analysis is a useful method for the analysis of the explosive welding. Using a numerical model, we obtain a better understanding of the factors that determine the quality of the joints. Also, the relationship between the process variable, physical parameters and identification of critical parameters can be expressed for acceptance or rejection of a welding process. In this study, the experiment was conducted to investigate the effects of numerical results on the interface microstructure. Numerical study was carried out by finite element analysis using ABAQUS software. Effects of numerical parameters such as pressure, dynamic collision angle and flyer impact velocity on the microstructure and morphology of the interface and correlation between the numerical parameters and microstructural properties of the interface would be discussed.

2. Materials and Methods

Sheets made of Inconel 718 in solution annealing condition and quenched-tempered hot-work AISI H13 steel were selected as flying and base plates, respectively. Before welding, hot-tool steel plates were processed with a heat treatment cycle as follows: they were first preheated in the temperature range of 350-550 °C for 2 hours. Then the plates were austenitized at a temperature of 1000 °C in the oven for 45 minutes. Then, they were quenched to 570 °C in the salt bath for 15 minutes and were transferred into the air. It was annealed at 520 °C for 3 hours and annealed again at 600°C for 3 hours for the second time then cooled in air to room temperature. The chemical compositions of the flyer and parent plates are given in Table 1. Flyer and parent plates were sequentially prepared with dimensions of 130mm × 130 mm × 3.2 mm and 100 mm × 100 mm × 10 mm, respectively.
Mechanical properties of the flyer and parent plates are

Table 1. The chemical composition (wt. %) of flyer and parent plates.

Elements	C	Si	Cr	Ni	Mo	Fe	Nb	Mn	V	Ti
AISI H13	0.42	1.05	5.09	0.12	1.14	Bal.	-	0.35	0.82	0.004
Inconel 718	0.06	0.02	18.55	Bal.	3.02	19.8	4.75	0.05	0.033	0.95

given in Table 2. It was proposed that the minimum percentage of the required elongation for explosive welding is 5% and the impact toughness of base metals should be more than 14 J [10]. According to Table 2, the percentage of the elongation of both base metals are more than 5 percent and also the impact toughness of both plates is more than 14 J. Therefore, the formation of cracks for explosive welding of dissimilar materials of AISI H13 and Inconel 718 is not predicted.

The explosive material was Amatol 90/10 (90% of Ammonium Nitrate and 10% of TNT). Detonation velocity and density of the explosive were 3100 m/s and 850 kg/m^3, respectively. The parallel arrangement was employed for the experiment (Fig. 1). The explosive was packed in the wooden boxes whose dimensions were the same as the dimension of the flyer plate. A C4 detonator was set on one end of the flyer plate. Setup was embedded in a sand pool on earth. In order to investigate the effects of explosive loading on bonding interface, the experiment and its parameters were designed and chosen by numerical simulations using ABAQUS/Explicit code. The Williamsburg-type equations of state were used to model explosive material. The Williamsburg equations of state were previously developed for low explosive mixture [15].

The numerical values such as impact velocity, dynamic collision angle and pressure were obtained from simulation. Mean impact velocity and dynamic collision angle are given in Table 3. Explosive ratio (R) in Table 3 denotes the mass of explosive per unit mass of the flyer plate. The Johnson-Cook equations [16] were used to model the behavior of the plates. The Johnson-Cook equations were described as:

$$\sigma = (A + B\,\varepsilon^{n})(1 + C ln\,\dot{\varepsilon}_{p})(1 - T^{(*m)}) \qquad \text{Eq. (1)}$$

, where ε equivalent to plastic strain is, $\dot{\varepsilon}_p$ is plastic strain rate for $\dot{\varepsilon}_0 = 1^{1}, T^{*} = \frac{T - T_{room}}{T_{melt} - T_{room}}$, T is absolute temperature for 0≤T*≤1 and A, B, C, n, m are constants. Constants in this equation are given in Table 4 for the materials used in this study.

Table 2. Mechanical properties of flyer and parent plates.

Materials	Elastic modulus (GPa)	Bulk modulus (GPa)	Hardness (Vickers)	Tensile strength (MPa)	Yield stress (MPa)	Density (kg/m^3)	Bulk sound velocity (m/s)	Elongation (%)	Impact toughness (J)
AISI H13	211	159.85	450	1346	606	7800	4527	7.8	22
Inconel 718	206	163.5	350	885	497	8190	4468	25.2	34

Table 3. Experimental characteristics of the set-up used with its corresponding numerical and microstructural results

Stand-off distance (mm)	Explosive ratio (R)	Mean Impact velocity (m/s)	Mean dynamic collision angle (Degree)	Interface morphology
3	3	610	12.43	Wavy with vortices

Table 4. The Johnson-cook equations parameter for the materials used in this study [22-24].

Materials	A (MPa)	B (MPa)	C	n	m	Melting temperature (K)	$\dot{\varepsilon}_0$ [s^{-1}]
Inconel 718	450	1700	0.017	0.65	0.13	1570	0.001
AISI H13	908.54	321.39	0.028	0.278	1.18	1760	0.001

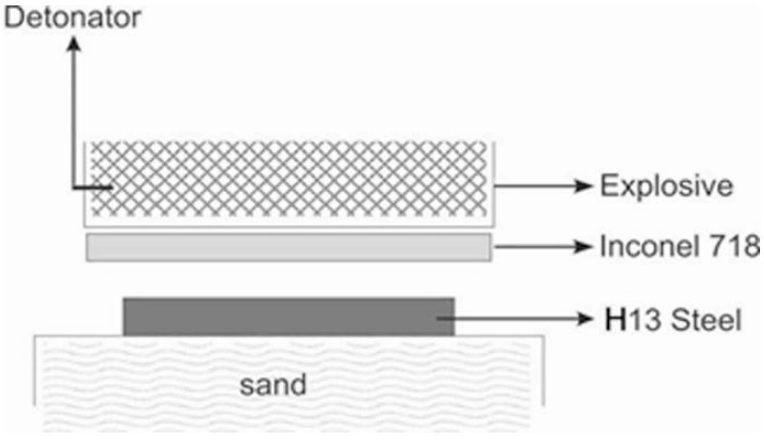

Fig. 1. Parallel arrangement of experimental setup for explosive cladding.

To reveal the microstructural aspects of the interface, the specimen was cut parallel to the detonation direction. The cross-section of the specimen was grounded with emery papers up to No. 1200 and polished with diamond paste. To investigate the microstructure, Nital etching solution (2%) and 60 ml HCl + 6 g $CuCl_2$ + 5 ml H_2O_2 etching solution were respectively used for steel and Inconel. The observation of the structural changes due to explosive cladding process was examined by optical microscope and scanning electron microscope. Energy-dispersive X-Ray spectrometry (EDS) analysis was also carried out. Micro hardness measurements of cladded metal were carried out with Duramin type micro hardness test machine with 50g loads, three different measurements were taken in distance of 25, 50, 75, 100, 200, 500 microns from the interface on both sides and the average values were reported.

Fig. 2 illustrates the welded samples under the ultrasonic inspection. Fig. 2 also represents an additional sectioned part of the flying plate of Inconel. Most of the samples had defects of lack of joints at the end of explosion that were mainly created due to the small size of plates and failing in fast separation of copper separators during the explosion, and the distribution of these defects was spotted as small concentrated areas at the corners of the joints and in some rare cases, as widespread distributions up to 20mm apart in the transverse axis of the samples. The rest of zones represented complete joints without failures and cracks from which specimens of qualitative tests were sampled.

3. Results and Discussions

3. 1. Simulation results

3. 1. 1. Pressure

Typical simulation stage of the process at an elapsed time of 23 μs was shown in Fig. 3.
Fig. 4 shows the typical pressure profiles at an elapsed time of 23 μs. It has been proposed that pressure has to be sufficiently high for a sufficient length of time to

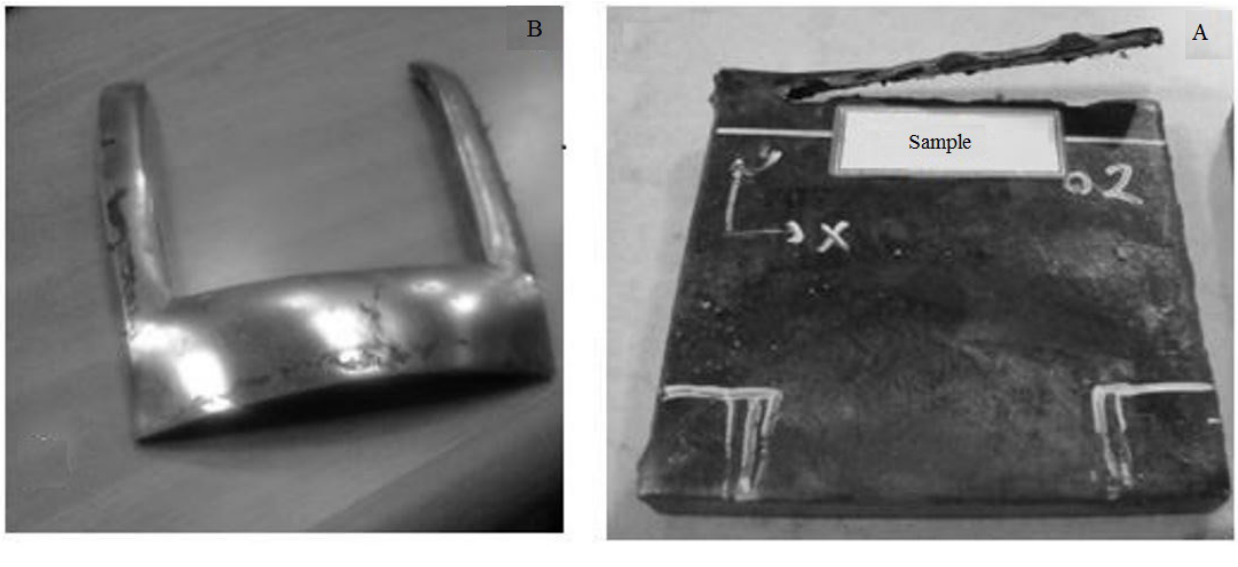

Fig. 2. a) Ultrasonic test connected and Non-Connected Areas b) Findings from the cutting Inconel flyer after the connection.

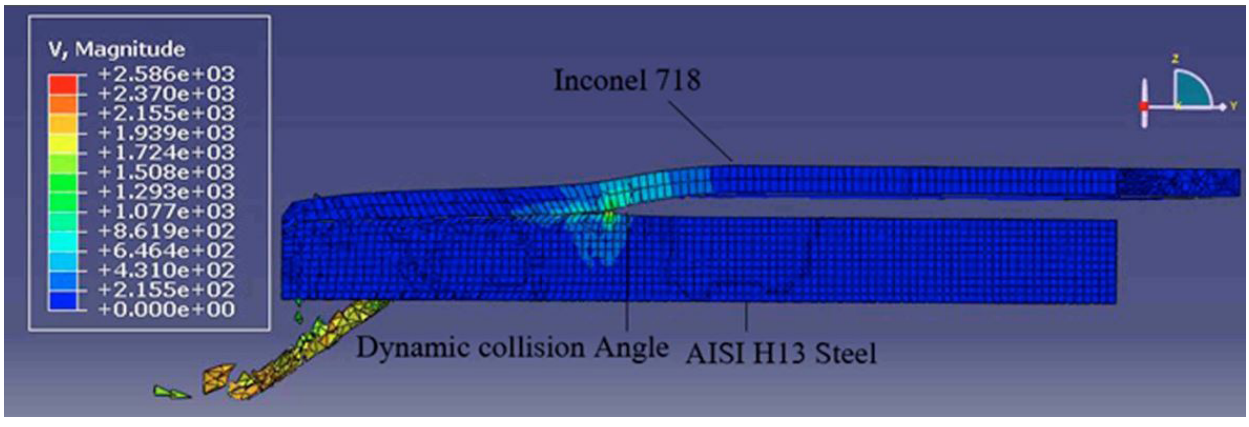

Fig. 3. Typical simulation stage of process at an elapsed time of 23 µs.

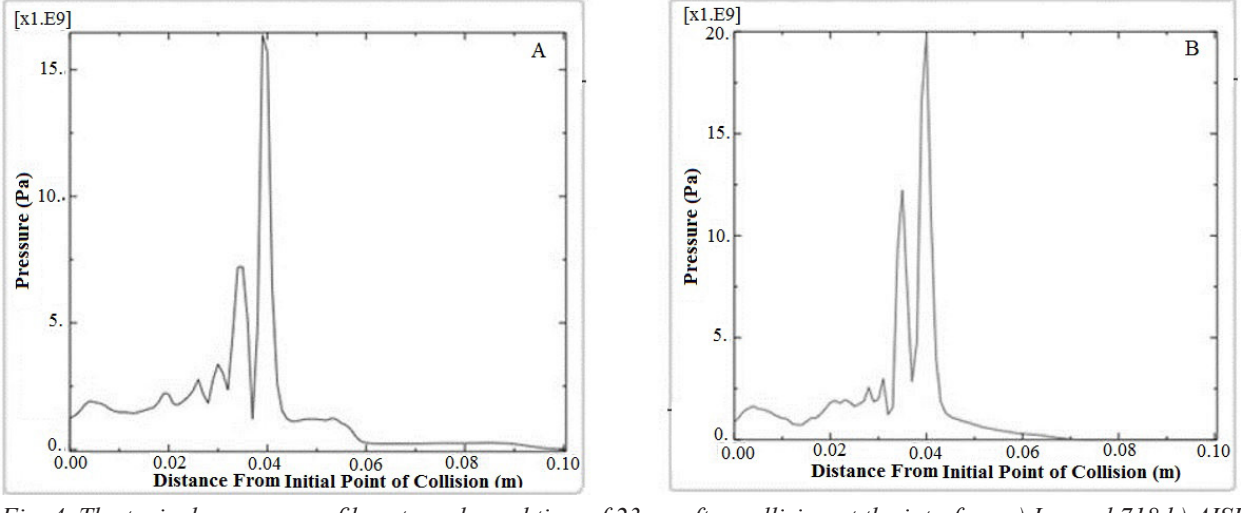

Fig. 4. The typical pressure profiles at an elapsed time of 23 µs after collision at the interface a) Inconel 718 b) AISI H13.

achieve inter-atomic bond and exceed the dynamic elastic limit of the material to ensure deformation of the metal surface into a jet [15, 16].

The highest pressure occurs at the collision point is in the order of GPa. The highest magnitude of pressure as shown in Fig. 4 is about15 GPa for Inconel side and 20 GPa for steel side .The maximum pressure is more than ten times of yield stresses of both alloys. This criterion was proposed by Blazynski [10] as the main condition required for bonding. The high pressure produced high localized plastic deformation at the interface. It can be assumed that the metal acts as a fluid in the interface and surface atoms are combined. Therefore, deformation of metal surface by shear wave velocity occurs.

3. 1. 2. Flyer Impact Velocity

Fig. 5 shows the typical flyer impact velocity profile at an elapsed time of 22 µs. The flyer plate was accelerated initially by a shock wave resulting from detonation pressure, and then by the expanding gaseous products of detonation [16]. Fig. 5 shows that flyer velocity increases from zero to its highest at the collision point and then the velocity reaches zero. The changes observed in the curves to the point of maximum are based on the reaction of collided surfaces. Mean flyer impact velocity was calculated and the result is tabulated in Table 3.The calculated velocity is higher than 350 m/s, which is the minimum flyer velocity required for bonding to take place that was proposed by Kowalewskij [15] equation.
Fig. 5. Typical flyer impact velocity profile at an elapsed time of 23 µs.

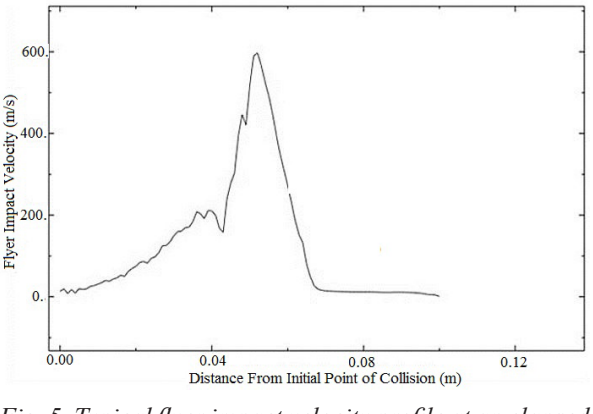

Fig. 5. Typical flyer impact velocity profile at an elapsed time of 23 µs.

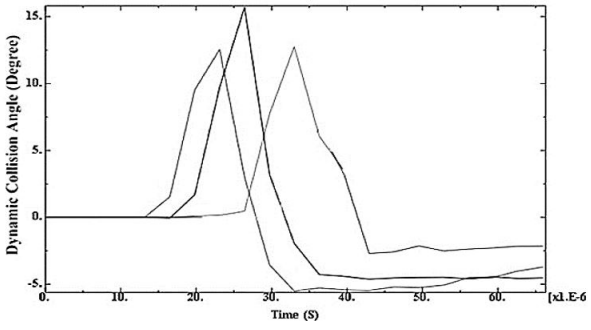

Fig. 6. Typical dynamic collision angle variations with advancing the collision point at different elapsed times.

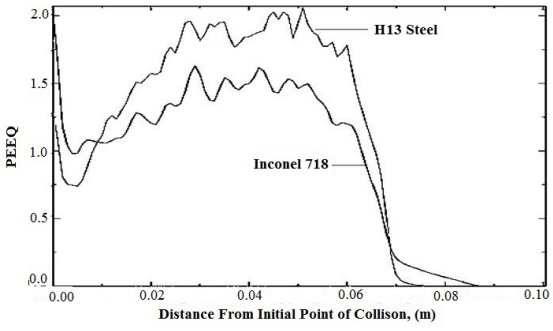

Fig. 7. Typical equivalent plastic strain profile at an elapsed time of 32 μs.

3.1.3. Dynamic collision angle

Typical dynamic collision angle variations with advancing the collision point at different elapsed times were depicted in Fig. 6. Fig. 6 shows that the dynamic collision angle is not constant. Dynamic collision angle increases with time by advancing the collision point then decreases again. It was proposed that by advancing the collision point, dynamic collision angle increased according to the plastic hinging and then decreased by reducing the stand-off distance. The result of this study is inconsistent with previous research [15]. Mean dynamic collision angle was calculated and the result was tabulated in Table 3.The calculated angle was higher than 7 degrees as the minimum impact angle required for the jet formation that was proposed by Wittman-Deribas-Stiver [25] equation.

3. 1. 4. Equivalent plastic strain

The typical equivalent plastic strain (PEEQ) profile at an elapsed time of 32 μs is shown in Fig. 7. It was shown in previous sections that pressure was in the order of GPa at the collision point (see Fig. 4), and impact velocity was reached its highest magnitude at the collision point (see Fig. [5]. The high pressure and velocity can give rise to producing high plastic deformation at the collision point which in turn produce large values of plastic strain (>1.5).The results also show that the value of the equivalent plastic strain (PEEQ) is reached its maximum at the collision point which indicates the maximum limit of deformation is approached.

3. 2. Microstructure study

Failure to control the consumed kinetic energy caused by collision leads to the creation of defective welding, brittle and phased molten castings at the joint interface. The consumed kinetic energy resulting from the potential energy of the explosion will determine the shape of the interface. Explosive welding of metals with high initial yield strength and high hardening strain rate is difficult. To solve this problem, an intermediate plate will be considered that should be thin with a high ductility, a high thermal conductivity, low yield strength and similar chemical analyses or in some cases, differ-

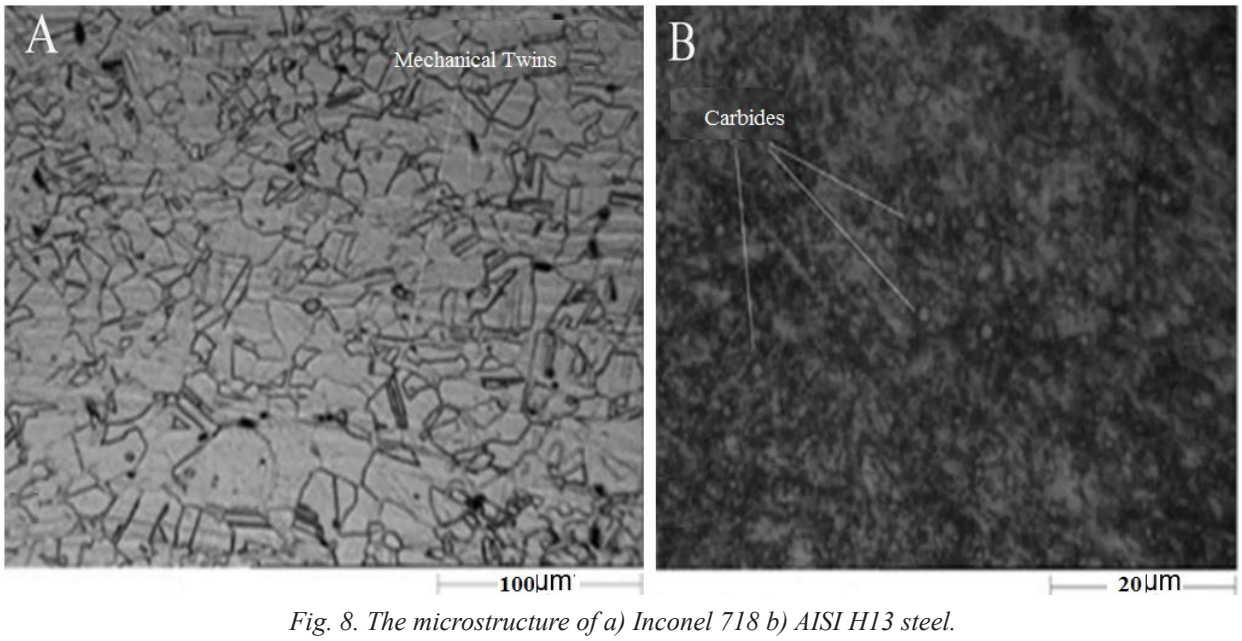

Fig. 8. The microstructure of a) Inconel 718 b) AISI H13 steel.

ent from the joint components to reduce the metallurgical problems of the joint. This intermediate page reduces the plastically deformed layer at the intersection that by reducing the kinetic energy of the flying plate, leads to reduced or no intermetallic compounds.
The microstructures of AISI H13 hot tool steel and Inconel 718 superalloy are respectively shown in Figs. 8a and 8b. Fig. 8a shows the superalloy microstructure which is mainly composed of austenite grains with mechanical twins and scattered fine carbides precipitations. Fig. 8b shows the steel microstructure which is mainly composed of tempered martensite with fine carbides precipitations.
Fig. 9a shows that bonding at the interface has a wavy with vortices morphology. It was proposed 26) that the wavy interface is produced due to oscillation in the jet flow. The degree of oscillation depends on the velocity of the collision.

The mean amplitude size of the formed waves was about 20 micron and the mean wavelength in the interface was about 73 micron. Fig. 9a shows a gradual change in the wavelength along the direction of welding which is due to a change in impact angle following the plates contact (see Fig. 6). Fig. 9 shows that the densities of twins increased at the interface. Moreover, slip bands were produced in the austenite grains. In low stacking fault free energy (SFE) face center cubic alloys such as Inconel 718, the dominant deformation microstructure is the occurrence of twins. The critical pressure required for twinning formation was proposed 12) to be in the order of 10 GPa. Fig. 4 shows that peak pressure in the vicinity of Inconel interface exceeds more than 15GPa and therefore it can be iterated that high pressure could facilitate plastic deformation through twining. Figs. 10 and 11 illustrate the SEM micrographs in the vicinity of Inconel superalloy interface. It can be clearly seen from Figs. 10 and 11 that twinning and slip are major plastic deformation mechanisms in austenite grains in order to accommodate the severe deformations that caused by the collision of the plates and traveling the shock wave in superalloy. Twinning and slip are two competing deformation mechanisms where temperature and strain rate dictate which of the two mechanisms will dominate. Lower temperatures and higher strain rates favor deformation by twinning [27]. Under the action of the stresses generated in the superalloy by the cladding process, displacement proceeds according to a basic mechanism, namely crystallographic slip. This mechanism proceeds in multiple planes in the case of polycrystalline materials such as in the case of Ni-based superalloys. Scanning electron microscope examination shows that according to activation of different slip systems, austenite grains strongly aligned and broken down and cellular microstructure was created (see Fig.11).The angles formed between the various slip lines observed within the grains with slip system 75-80°. In this study, the superalloy has an f.c.c microstructure. In the case of materials with f.c.c microstructure, the principal slip systems are of the type <110> {111} [11].

Under the explosive welding conditions, the high-velocity oblique collision produces high temperature, high pressure, high plastic strain (see Figs. 4, 7) and high strain rate near the collision point 28). For low stacking fault free energy metals, discontinuous dynamic recrystallization occurs by local rapid cycles of strain hardening and is facilitated by the twining 29). Fig. 9a shows that grains are refined in some areas near the interface of Inconel superalloy according to discontinuous dynamic recrystallization. As the superalloy was

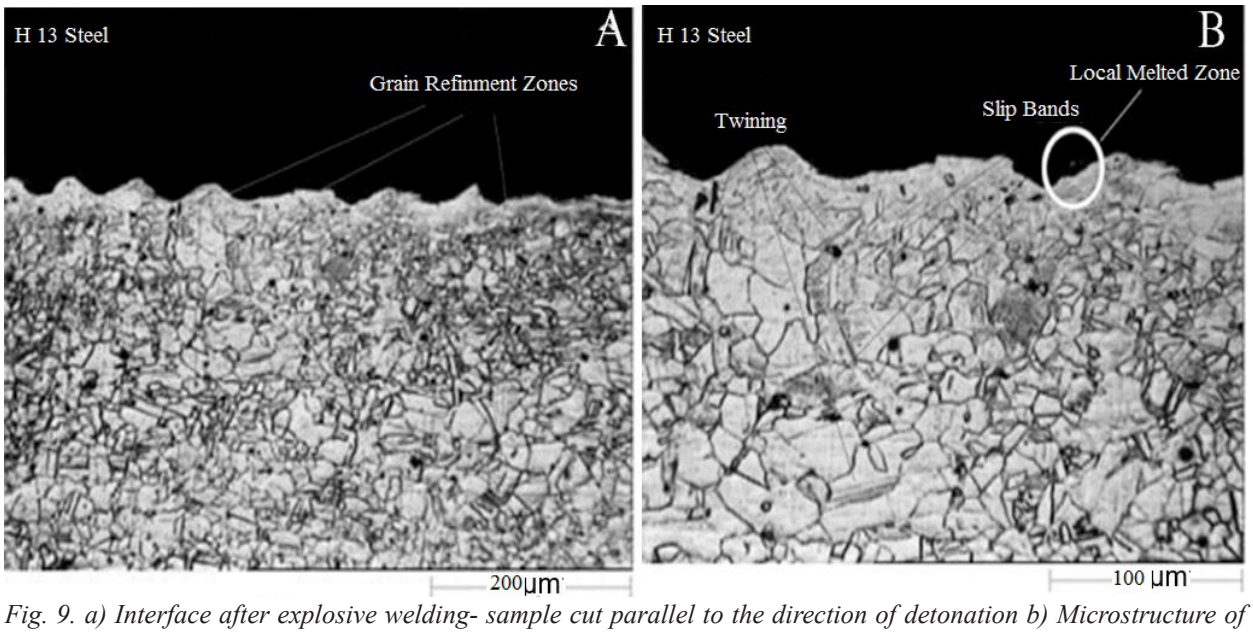

Fig. 9. a) Interface after explosive welding- sample cut parallel to the direction of detonation b) Microstructure of Inconel 718 in the vicinity of interface.

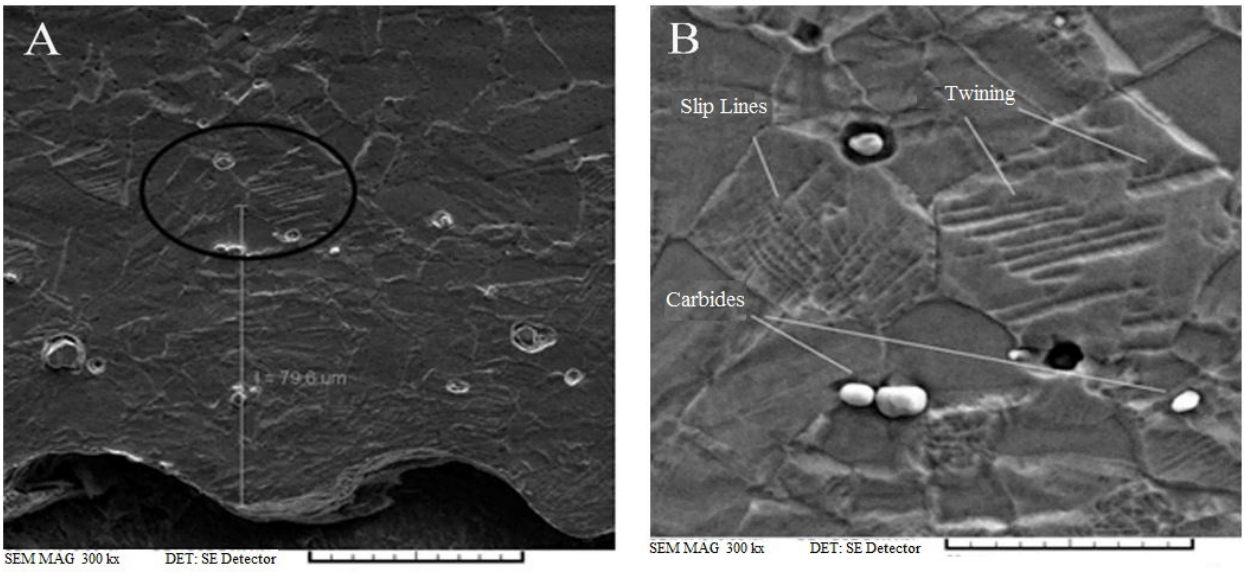

Fig. 10. SEM micrograph of Inconel 718 microstructure in the vicinity of the interface a) selected area in 79 micron distance from interface b) deformation twins formations.

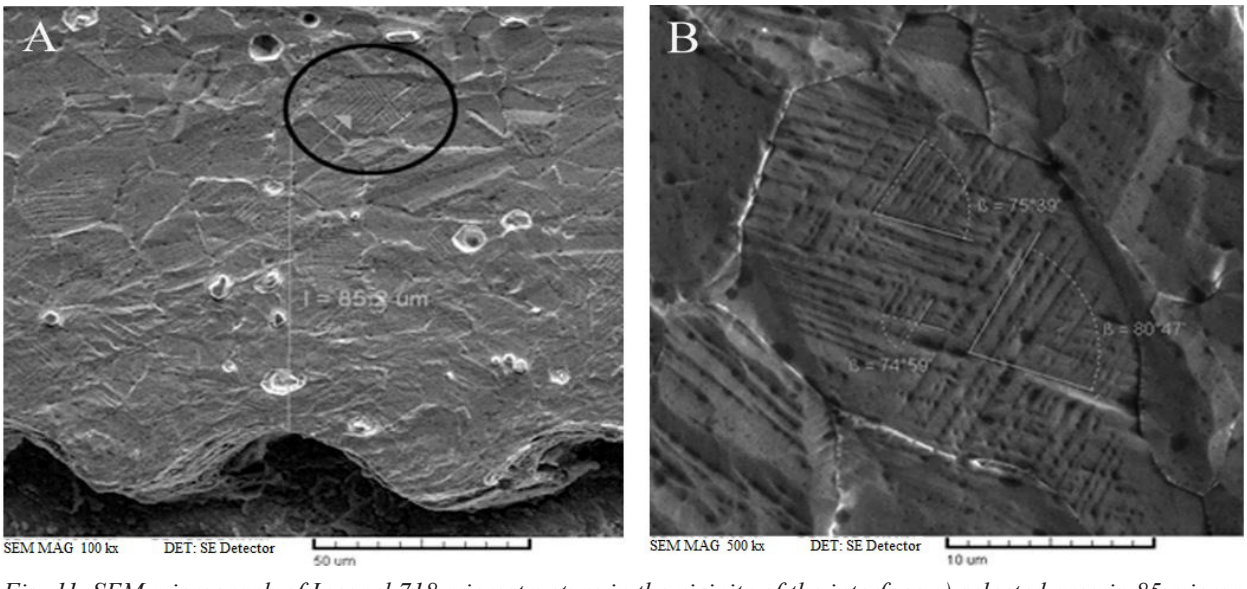

Fig. 11. SEM micrograph of Inconel 718 microstructure in the vicinity of the interface a) selected area in 85 micron distance away from the interface b) highly plastic deformed austenite grain.

deformed at a high temperature, new grains were nucleated and grown within the deformed grains. Since the process was too fast, there was no time for grain growth to the larger size.

Solidified melts were also observed in front of vortices as shown in Figs.9b and 12. A typical backscatter scanning electron micrograph is shown in Fig. 13.In explosive welding, metal-metal and metal-solidified melt could be generated at the interface. Vortices were formed under excessive pressure. The vortex can exhibit local melting zone in some sections of weld interface due to adiabatic heating of trapped jet inside vortices at the front slope of waves. The molten zone is surrounded by relatively cold metal and subjected to a very high cooling rate in the order of 105-107 K/s 25).

Fig. 13 shows that the interface was outlined by sharp transition between two materials but locally melted zone in the form of thin pockets was produced in front of waves. The increase of temperature at the collision point may be more enhanced if there is a high difference between the thermal conductivity of flyer and parent plate materials. Since the thermal conductivity of Inconel 718 (11.4 $W\text{-}m^{-1}\text{-}K^{-1}$) was lower than that of AISI H13 steel (28.4 $W\text{-}m^{-1}\text{-}K^{-1}$), therefore upon solidification of the melting pockets, the heat was conducted from melted zone to Inconel 718 and melts pockets were observed more in the interface of Inconel 718 than in that of AISI H13 steel.

EDS spot analysis was also carried out on the melting pockets region. EDS spot analysis of the locally melted

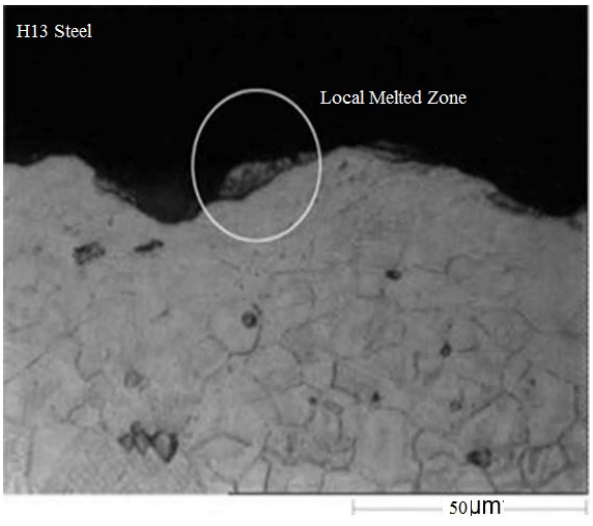

Fig. 12. Higher magnification micrograph of selected local melted zone at the interface of Fig. 9b.

zone is shown in Fig. 14. Results showed that the chemical composition of melted zone consisted of AISI H13 and Inconel 718 (see Fig. 14c) due to circular movement and stirring of molten materials and mixing of both flyer and base plates [25].

3. 3. Micro hardness study

Microhardness measurement was made across the interface of Inconel 718-AISI H13 steel. The Vickers hardness of Inconel 718 and H13 steel was 350 Hv and 450 Hv, respectively. The variation of hardness with distance from the interface is shown in Fig. 15.The maximum hardness occurred close to the interface and the hardness decreased with the distance away from the interface. The change of hardness was found to be more severe in superalloy than in steel. The results showed

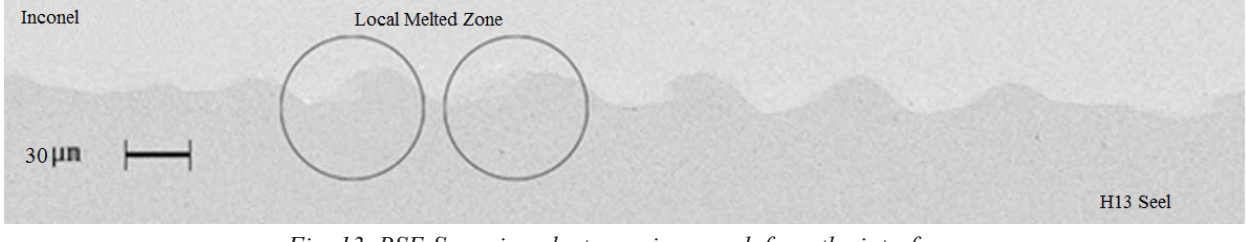

Fig. 13. BSE-Scanning electron micrograph from the interface.

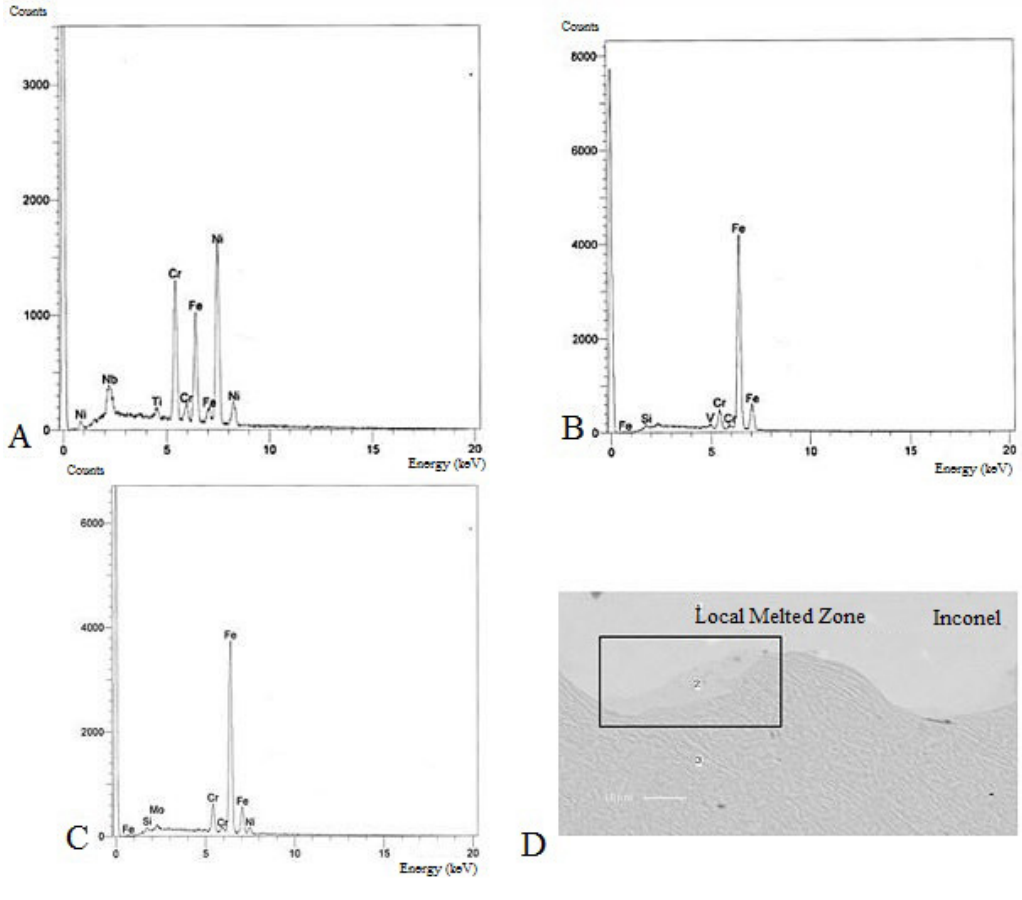

Fig. 14. EDS analysis a) From Inconel side (point no.1), b) From H13 steel side (point no.3), c) From local melted zone (point no.2), d) Analyzed section.

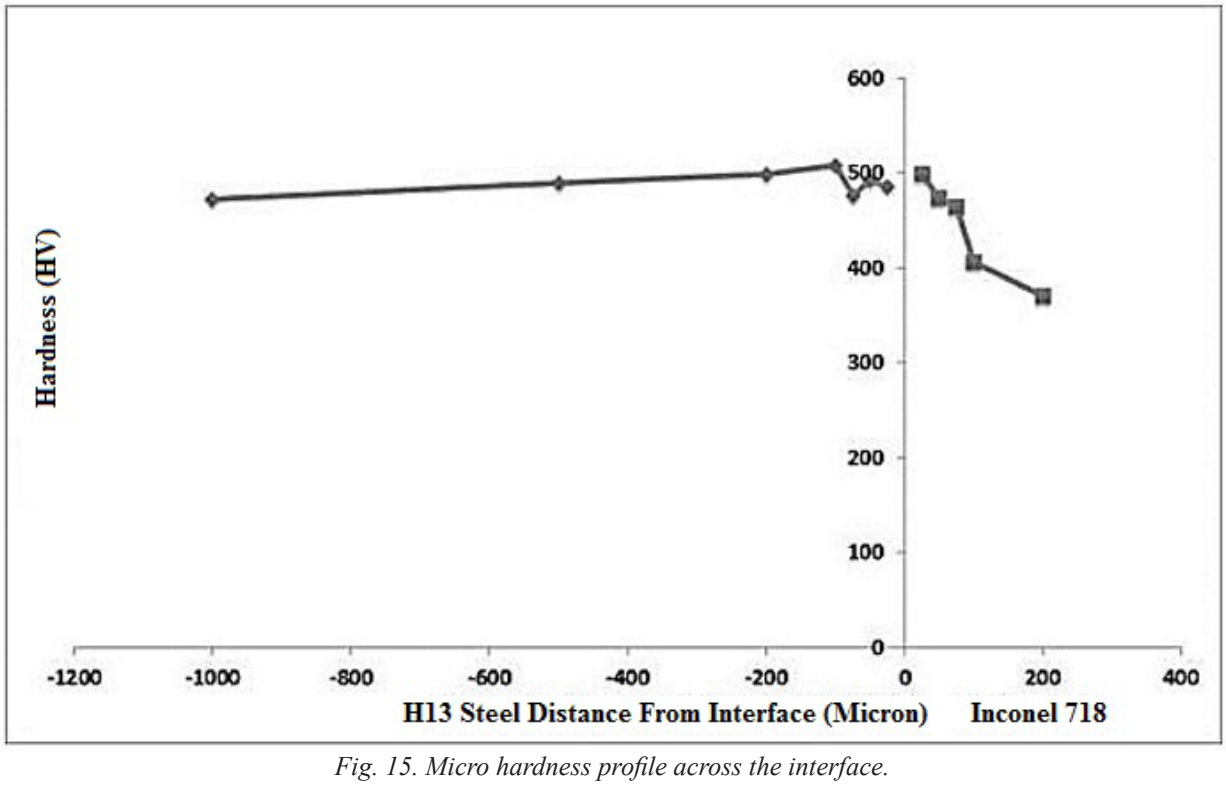

Fig. 15. Micro hardness profile across the interface.

that at a distance of 25 micron from the interface, the hardness was measured to be 499 Hv for Inconel and 486Hv of H13 steel. Fig. 4 shows that the pressure reached the maximum level at the interface, as a result, the hardness increased near the interface due to the high level of plastic deformation adjacent to the weld interface and also grain refinement. Twin formation and slip bands development in the Inconel superalloy would contribute to the plastic deformation hardening effect (see Figs. 9-11).

4. Conclusion

- Wavy with vortices morphology between Inconel 718 and AISI H13 Steel were produced.
- Simulation results showed that maximum values of pressure and impact velocity were obtained at the collision point and dynamic collision angle was not constant across the collision points.
- Peak pressure in the vicinity of the interface exceeded more than 15GPa which facilitated plastic deformation by twining.
- Twining and slip were the major plastic deformation mechanisms in austenite grains to accommodate the severe deformations that caused by traveling the shock wave from the superalloy.
- The difference between thermal conductivity of Inconel 718 and AISI H13 caused that thin melts pockets were observed more in the interface of Inconel 718 than in that of AISI H13 steel.
- Results showed that the change of hardness was more severe in superalloy than in steel.

References

[1] S. A. Rizvi and T. I. Khan: Trib. Int., 32(1999), 567.
[2] T. I. Khan, S. A. Rizvi and K. Matsuura: Wear., 244(2000), 154.
[3] C. Bournicon: Traitements Thermiques., 246(1991), 70.
[4] R. Davis: Specialty Handbook, Tool Materials, ASM, (1995).
[5] F. Nippes: Metals Handbook, Welding, Brazing and Soldering, ASM, (1991).
[6] P. Fournier and A. Bennani: Bulletin du cercle d' Etudes des Metaux., 18,17.1, (2000).
[7] J. N. Dupont, C. V. Robino and A. R. Marder: Weld. J., 77(1998), 417.
[8] J. N. Dupont, C. V. Robino, A. R. Marder, M.R. Notis and J. R. Michael: Meta. Mater. Trans. A., 29, (1998), 2785.
[9] G. A. Knorovsky, M. J. Cieslak, T. J. Headley, A.D .Romig and W.F. Hammetter: Meta. Mater. Trans. A., 20(1989), 2149.
[10] T. Z. Blazynsky: Explosive forming welding and compaction, Applied Science Publisher LTD, (1983).
[11] S. Ettaqi, L. Langlois and R. Bigot: Surf. Coat. Tech., 202(2008), 3306.
[12] L. E. Murr, E. Ferreyra, S. Pap, J. M. Rivas, C. Kennedy, A. Ayapu, E. I. Garcia, J. C. Sanchez, W. Huang and C.S.Niou: Mat. Character., 37(1996), 245.
[13] A. Durgutlu, H. Okuyucu and B. Gulenc: Mater. Des., 29(2008), 1480.
[14] M. Acarer, B. Gulenc and F. Findik: Mater. Des., 24(2003), 659.
[15] S. A. A. Akbari Mousavi and S. T. S. Al-Hassani:

J. Mech. Phys. Sol., 12(2005), 251.
[16] S.A.A. Akbari Mousavi and S.T.S. Al-Hassani: Mater & Des., 29, (2008), 1.
[17] S.A.A. Akbari Mousavi, S.J. Burley and S.T.S. Al-Hassani: Imp. Eng., 31(2005), 719.
[18] S.A.A. Akbari Mousavi, S.T.S. Al-Hassani, W. Byers Brown, and S. J. Burley: Propellants, Explosives, Pyrotechnics, 29(2004), 188.
[19] S.T.S. Al-Hassani, M. Chizari, and L. M. Barret: Mate. Proc. Techn., 209(2009), 445.
[20] F. Grignon, D. Benson, K. S. Vecchio and M. A. Meyers: Imp. Eng., 30(2004), 1333.
[21] S.A.A. Akbari Mousavi, S.T.S. Al-Hassani and S. J.Burley: Int. J. Imp. Eng., 31(2005), 719.
[22] K. N. Singh, R. Clos,U. Schreppel, P. Veit, A. Hamann, D. Klingbeil, R. Sievert and G. Künecke: Technische Mechanik., 23(2003), 205.
[23] E. Uhlmann, M. Graf von der Schulenburg and R. Zettier: CIRP. Manu. Tech., 56, (2007), 61.
[24] H. Yan, J. Hua and R. Shivpuri: Mater. Des., 28(2007), 272.
[25] S.A.A. Akbari Mousavi and P. Sartangi, Mater. Des., 30(2009), 459.
[26] J. Song, A. Kostka, M. Veehmayer and D. Raabe: Mat. Sci. Eng. A., 528, (2011), 2641.
[27] C. H. Ambler: Ph. D Thesis, the University of Texas at El Paso, (2005).
[28] Y.B. Yana, Z.W. Zhang, W. Shen, J.H. Wang, L.K. Zhang and B.A. Chin: Mat. Sci. Eng. A., 527(2010), 2241.
[29] F. Montheillet and J. P .Thomas: Metallic materials with high structural efficiency, Kluwer academic publisher, (2004), 357.